



Investigation of The Effect of Radius of Curvature on Buckling Load in Thin-Walled Beams

Cenk YANEN*

Firat University, Mechanical Engineering Department, cyanen@firat.edu.tr, Orcid No: 0000-0002-5092-8734

ARTICLE INFO

Article history:

Received 25 October 2024
Received in revised form 25 November 2024
Accepted 29 November 2024
Available online 23 December 2024

Keywords:

buckling, thin-walled beam, post-buckling, finite element analysis

Doi: 10.24012/dumf.1573700

* Corresponding author

ABSTRACT

This study examines the effect of curvature radius on the buckling behavior of thin-walled beams, which are commonly used in aerospace, automotive, and structural engineering due to their high strength-to-weight ratios. The buckling phenomenon, which represents a critical failure mode for thin-walled hat-shaped structures, was investigated under axial loading through the utilization of numerical methods. A nonlinear analysis was conducted using ANSYS Workbench to model three distinct geometries with varying curvature angles and identical dimensions. The models were subjected to analysis in order to ascertain the critical buckling loads and reaction forces at a displacement of 1 mm, with a particular focus on both nonlinear and post-buckling behavior. Given its importance in structural applications, Aluminum Alloy NL was selected as the material. The eigenvalue buckling analysis identified the critical loads for the first ten modes, revealing that models with higher curvature angles demonstrated more stable buckling characteristics, whereas those with smaller angles were more prone to local deformation. A post-buckling analysis was conducted to ascertain the nonlinear load-bearing capacities of these structures.

Introduction

Hat-profile structural elements are of critical importance in the design of thin-walled structures in engineering, providing stability under a variety of loading conditions. One of the most notable characteristics of these structures is their capacity to combine lightweight properties with high strength. Hat profiles are commonly employed in fields such as aerospace, automotive, marine, and construction, as they effectively distribute forces across a wide surface area. These elements demonstrate high resilience against impact loads, rendering them particularly well-suited for critical functions such as energy absorption in the event of a collision. The utilization of such profiles in aircraft fuselages, wing structures and rocket components is intended to ensure the maintenance of structural integrity while simultaneously reducing weight. The aforementioned structural elements in aircraft fuselages serve to enhance resistance to dynamic loads, including pressure, tension, and impact, which are experienced during flight [1]–[3]. In the automotive industry, hat-shaped profiles are employed in the construction of chassis structures and in the context of crash testing scenarios. Their function is to absorb impact energy, thereby enhancing passenger safety [4]–[6]. One of the most significant engineering challenges faced by hat-

shaped structural elements is that of buckling. Buckling occurs when a structure loses stability under axial loads, resulting in sudden deformation, which can be particularly hazardous for thin-walled structures. It is of paramount importance to enhance the resistance of structural elements to buckling in order to ensure safety and efficiency. The buckling process is typically analyzed in three stages: pre-buckling, critical buckling and post-buckling. In the pre-buckling stage, the structure displays elastic behavior in response to the applied load and remains stable. Upon reaching the critical buckling stage, the structure experiences a sudden loss of stability, resulting in the onset of deformations. In the post-buckling stage, the structure may continue to bear loads, but the deformations that occur at this stage are permanent and significantly impact the structure's durability. In sectors such as aerospace and automotive, the load-bearing capacity of a structure following buckling is regarded as a pivotal aspect of the design process [7], [8]. The curvature angle of hat-shaped structural elements represents a pivotal parameter that exerts a direct influence on the buckling behavior of such elements. Variations in curvature angle have a direct impact on both the critical buckling load and the post-buckling load-bearing capacity of the structure. In a study conducted by Masood et al., the post-buckling behavior of thin

composite stiffened panels employed in the construction of aircraft fuselages was subjected to experimental investigation. The buckling and post-buckling performance of thirteen panels, designed with various stiffener configurations (T-type, I-type, and J-type), were examined in order to gain insight into the effects of these configurations on the panels' structural behavior [9]. The buckling and post-buckling behaviors of composite panels with M-type stiffeners were investigated by Liu et al. The mechanical stabilities of panels commonly used in aircraft were determined using optical measurement methods and the finite element method [10]. In a study conducted by Wang et al., the stability behaviors of hat-stringer stiffened composite panels were examined both experimentally and through numerical analyses. Two test panels were produced, and the buckling load and ultimate load-carrying capabilities of these panels were determined numerically and compared with experimental results [11]. Hou et al. conducted impact tests on hat-shaped T-joints with weights dropped at three different impact velocities. A nonlinear finite element analysis was conducted to predict the damage and energy dissipation characteristics [12]. The buckling and post-buckling behaviors of hat-stringer reinforced composite flat panels subjected to axial compression were investigated by Mo et al. Based on the experimental data, the stability and deformation processes of the reinforced panel and the hat-stringer were analyzed. To assess the suitability of the hat-stringer section, five different models were evaluated using ABAQUS software [13]. The effects of curved surface composites under impact loads were investigated in a study by Albayrak et al., with a particular focus on their impact on energy dissipation [14]. Hat-shaped structural elements demonstrate high durability not only against axial loads but also against impact and pressure loads. In particular, these profiles are effective in absorbing impact energy while maintaining structural stability in aircraft fuselages. The accurate analysis of both buckling and post-buckling behaviors is essential for ensuring structural stability.

In this context, a precise understanding of the effects of curvature angle is essential for the optimization of structures. In this study, the buckling and post-buckling behaviors of hat-shaped samples with three different curvature angles were investigated numerically using the same geometries employed in the work by Albayrak et al. [14]. Subsequent to the buckling analysis, a post-buckling analysis was conducted to ascertain the load-carrying capacity of the structures in question following the buckling event. Nonlinear analyses conducted using ANSYS Workbench software facilitated a comprehensive assessment of the influence of curvature angle on structural performance.

Material and Method

This study examines the buckling behavior and post-buckling responses of hat-shaped structural elements under varying curvature angles through the use of numerical methods. The profiles under examination are defined by a hat-shaped geometry, which is a prototypical example of thin-walled structures, and were analyzed using a nonlinear

material model. This section presents the sample geometry, material properties, boundary conditions, and the applied numerical analysis methods.

Model Geometry and Material Properties

In the study, hat-shaped models with a fixed sample width ($w = 150$ mm), fixed wall thickness ($t = 1$ mm), and fixed sample height ($h = 25$ mm) were examined. The length of the samples was fixed at $l = 200$ mm, and three distinct curvature angles were employed. For illustrative purposes, the model geometry is depicted in Figure 1. The numerical analysis was conducted using the Aluminum Alloy NL material, which is available in the ANSYS Workbench library. The selected material's mechanical properties are presented in Table 1.

Table 1. Mechanical properties of Aluminum Alloy NL [15]

Material properties	Value
Density (kg/m ³)	2770
Young's Modulus (Pa)	7.1E+10
Poisson's Ratio	0.33
Bulk Modulus (Pa)	6.9608E+10
Shear Modulus (Pa)	2.6692E+10
Yield Strength (Pa)	2.8E+08
Tangent Modulus (Pa)	5E+08

Numerical Analysis and Boundary Conditions

Transformations in the deformation characteristics of numerous elements subjected to loading can result in the destabilization of the deformation state, thereby prompting the system to seek a new stable state. The stable state of a system is defined by its capacity to predict the post-deformation condition, whereas an unstable state is characterized by uncertainty following deformation. The analysis of perfect plates is conducted within the framework of the theory of small deformations, with the assumption that there is no midplane deformation of the plate element due to loading. In contrast, imperfect plates are examined in accordance with the "Great Deformation Theory of Plates," as developed by Von Karman. This theory takes into account the shape changes occurring in the midplane of the differential element during the analysis. In this study, an eigenvalue buckling analysis was conducted to determine the critical buckling loads for the first ten modes of the models. The boundary conditions employed in the analysis are depicted in Figure 2. The results of the analysis yielded load multiplier values for the first ten modes, which were then employed in the calculation of critical buckling loads using the following equation:

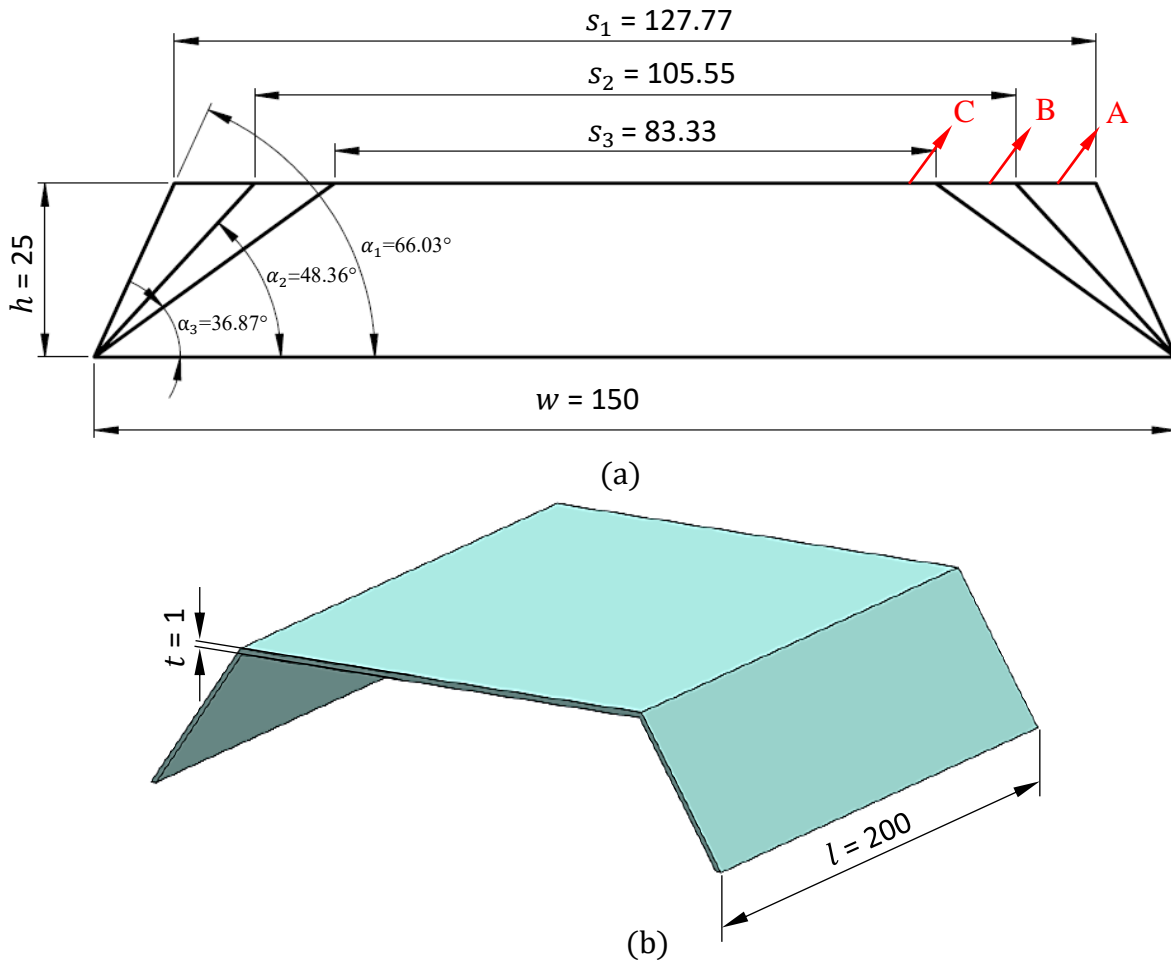


Fig. 1. Model geometries a) dimensions [14] b) solid model

$Critical\ buckling\ load\ (N) = Load\ multiplier * Force\ applied\ (N)$

In this study, a post-buckling analysis of a hat-shaped plate was conducted using the ANSYS Workbench. A nonlinear buckling analysis was conducted using both the static structural and eigenvalue buckling modules. The results of a previous eigenvalue buckling analysis of the stiffened plate were incorporated into the static structural module to investigate post-buckling behavior. A displacement range of 1 mm was applied to analyses the post-buckling response and identify the load at which collapse occurs. In the course of the analysis, the scale factor value was selected to be 0.004. The boundary conditions utilized in the numerical analysis are illustrated in Figure 3.

Results and Discussion

The buckling analysis revealed that the buckling behaviors of the three models differed due to their distinct geometric properties. Model A exhibited a more uniform and centralized buckling shape due to its wide upper surface (127.77 mm) and large curvature angle (66.03°). In the initial mode, the distribution of buckling exhibited greater uniformity, whereas higher modes demonstrated a tendency towards localized deformation. Model B, with a narrower

upper surface (105.55 mm) and a lower curvature angle (48.36°), exhibited a more intricate and undulating buckling behavior. The fluctuations observed from the third mode onward indicate that this structure was subjected to greater localized deformation due to its lower curvature angle. Model C, distinguished by the narrowest upper surface (83.33 mm) and the lowest curvature angle (36.87°), exhibited the most intricate buckling behavior. In the initial mode, smaller cellular structures were observed, while pronounced fluctuations occurred in subsequent modes. This outcome demonstrates that the low curvature angle and narrow upper surface result in heightened localized deformation during buckling.

Figure 5 presents a comparative graph of the critical buckling loads obtained for the initial ten modes following the non-linear buckling analysis. Upon examination of the variation in critical buckling loads among the modes, a distinct trend difference is observed. In the initial three modes, Model C exhibits the highest buckling loads. However, as the modes progress, this ranking shifts to $B > A > C$. The observation that Model C, which has the smallest curvature angle, endures higher buckling loads in the initial three modes suggests that structures with lower curvature angles demonstrate enhanced rigidity and resistance to minor deformations.

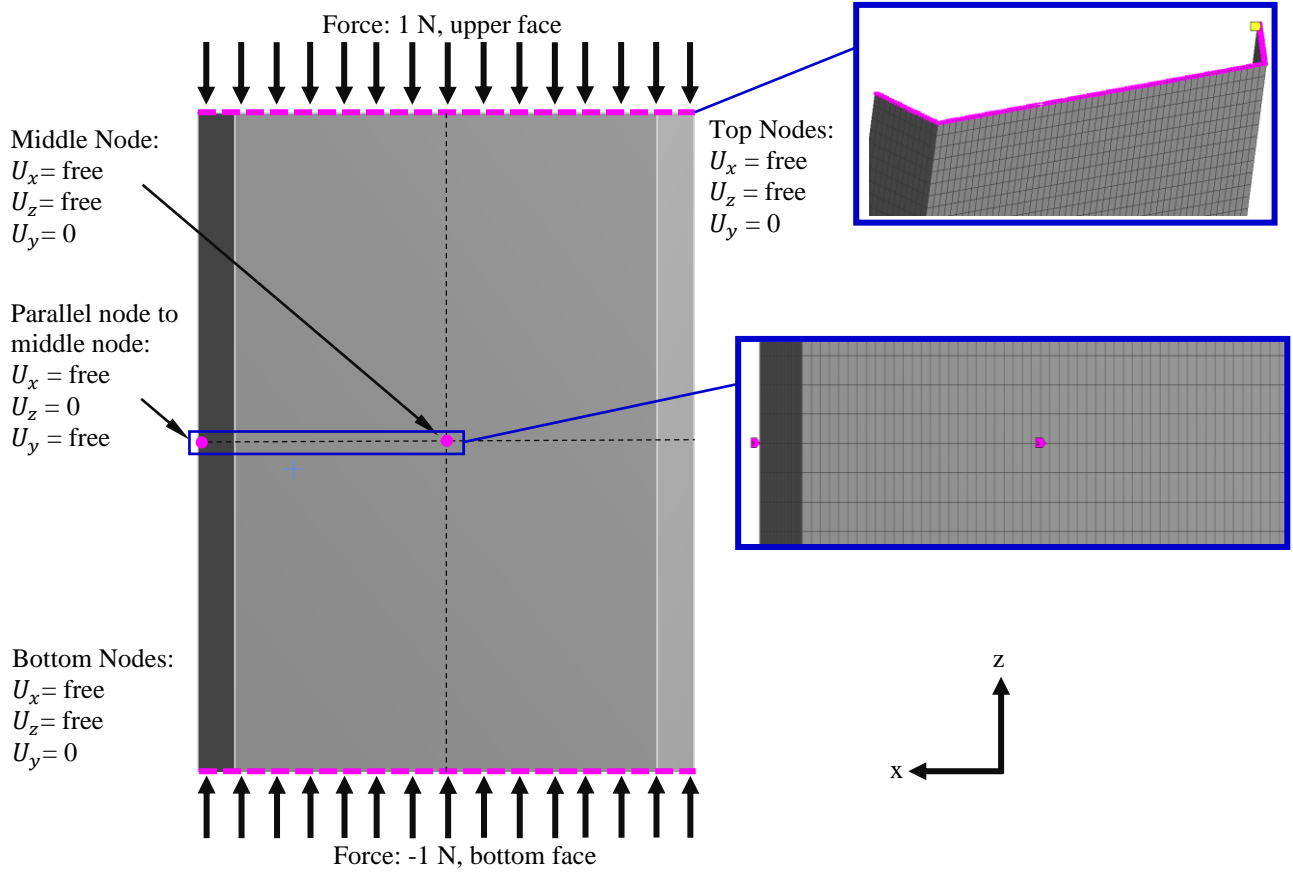


Fig. 2. Eigenvalue Buckling analysis boundary conditions

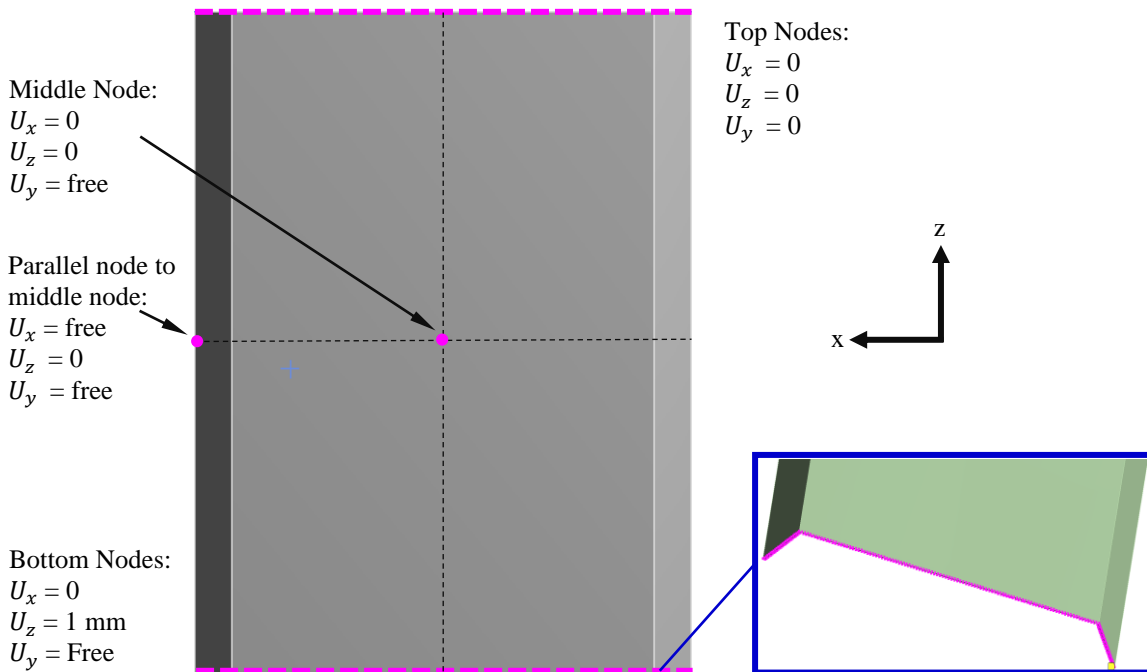


Fig. 3. Post-buckling analysis boundary conditions

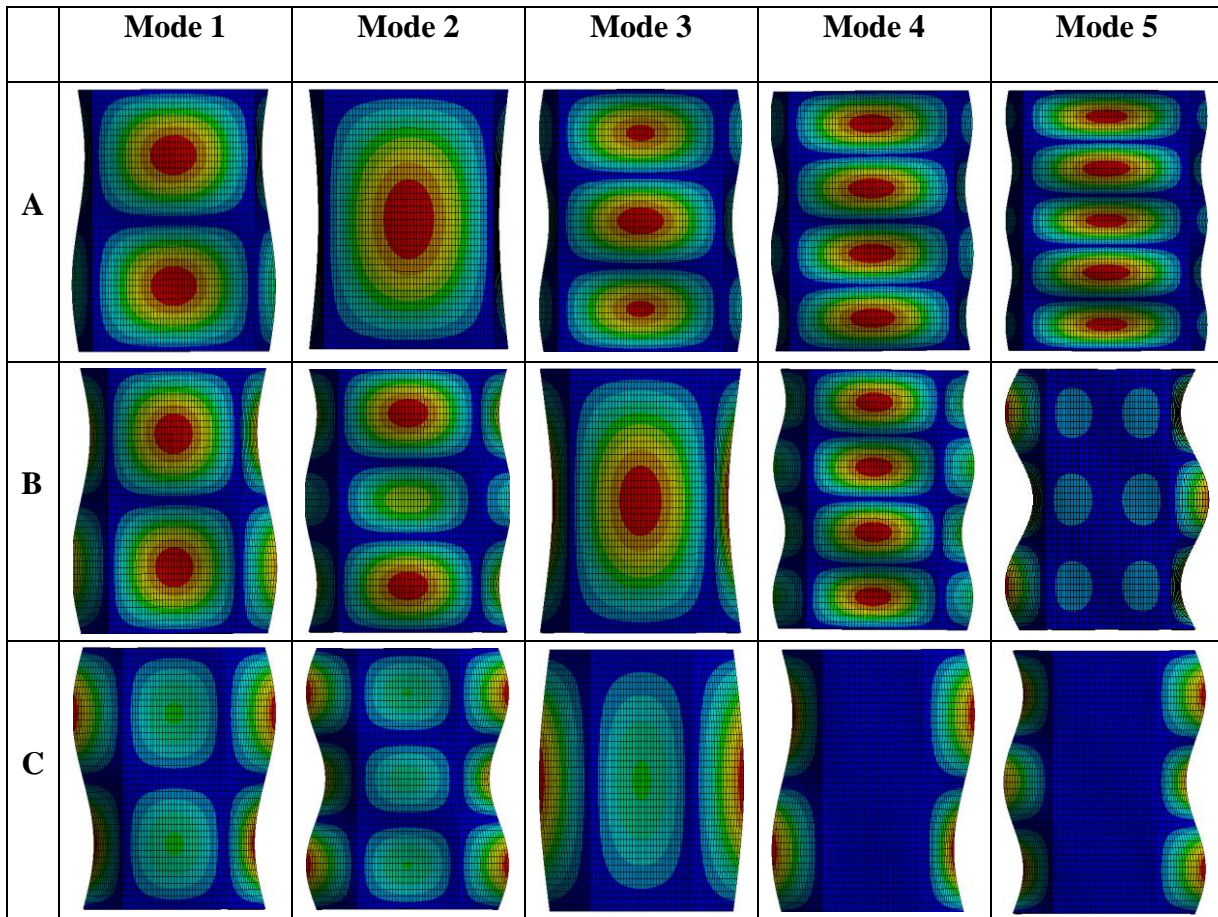


Fig. 4. The first 5 mode shapes of models A, B and C

The Model A's larger curvature angle results in a more flexible structure, enabling it to withstand lower buckling loads. In the fourth mode, Model B demonstrates superior performance, which can be attributed to its medium curvature angle. The occurrence of complex buckling modes serves to elucidate the stability conditions operative in disparate regions of the structures. During this phase, while Model C's high performance in the initial modes declines, Model B maintains a more balanced performance. In the fifth and tenth modes, it has been determined that the large curvature angle of Model A contributes to its greater resilience against buckling. As advanced modes represent complex buckling modes, larger curvature angles facilitate a more uniform distribution of the buckling load, thereby enabling Model A to withstand higher buckling loads. These findings demonstrate that the mode number and curvature angle have a complex interaction with regard to buckling loads, underscoring the importance of considering these loads in different modes during the structural design phase to ensure the creation of optimized and safe structures.

The load-end shortening graph, obtained from the post-buckling analysis, is presented in Figure 6. Upon examination of the graph, it can be observed that the initial increase in load corresponds to a linear relationship with the shortening of the end section, indicating that the structure is operating within its elastic region. This demonstrates that

the structural element functions elastically, and as the load magnitude increases, the deformation also increases in proportion.

This linear relationship persists up to a load value of approximately 4000 N, after which a nonlinear behavior is observed. This suggests that the structural element has exceeded its elastic limit and is approaching a state of instability. At this point, the stability of the structure is compromised, and deformation accelerates. It is noteworthy that the load reaches its peak between 0.6 and 0.7 mm and then begins to decline. This indicates that the critical buckling load has been exceeded, resulting in a transition to an unstable state. The observation that increases in load result in significant deformations despite minimal changes indicates a reduction in the structure's rigidity and a complexity in post-buckling behavior.

Notwithstanding the geometric discrepancies among the models, the load-deformation behaviors remain largely analogous, thereby indicating that the models do not exhibit appreciable differences in overall stability and rigidity. The maintenance of fundamental geometric parameters, such as base width and height, has been identified as a primary factor influencing the resistance to buckling. Nevertheless, alterations in the radius of curvature have led to minor discrepancies in peak load capacity and slight divergences in post-buckling behavior.

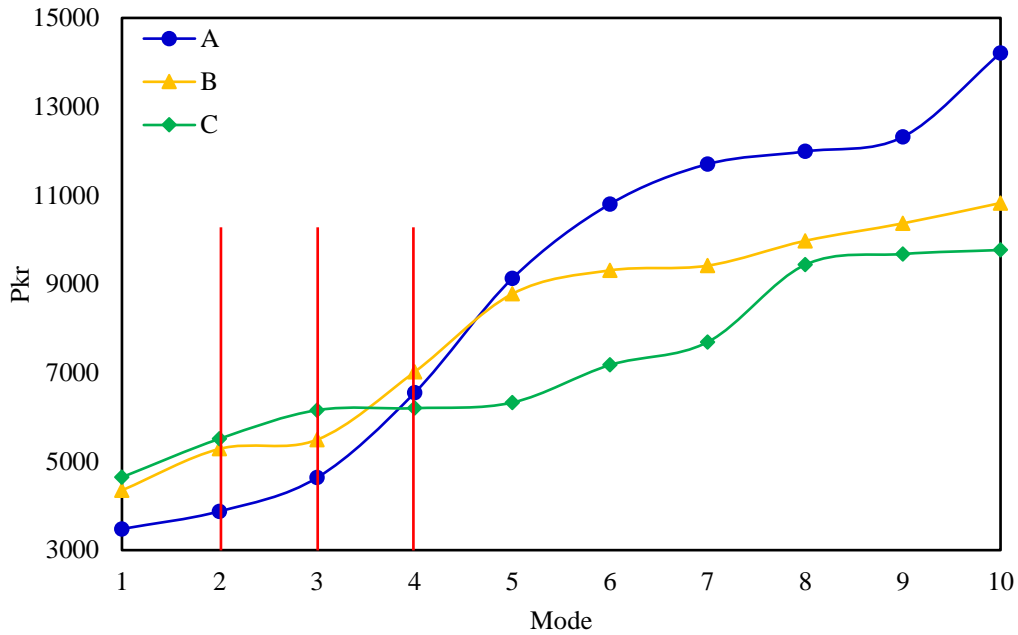


Fig. 5. Comparison of critical buckling loads in the first 10 modes of models A, B, and C

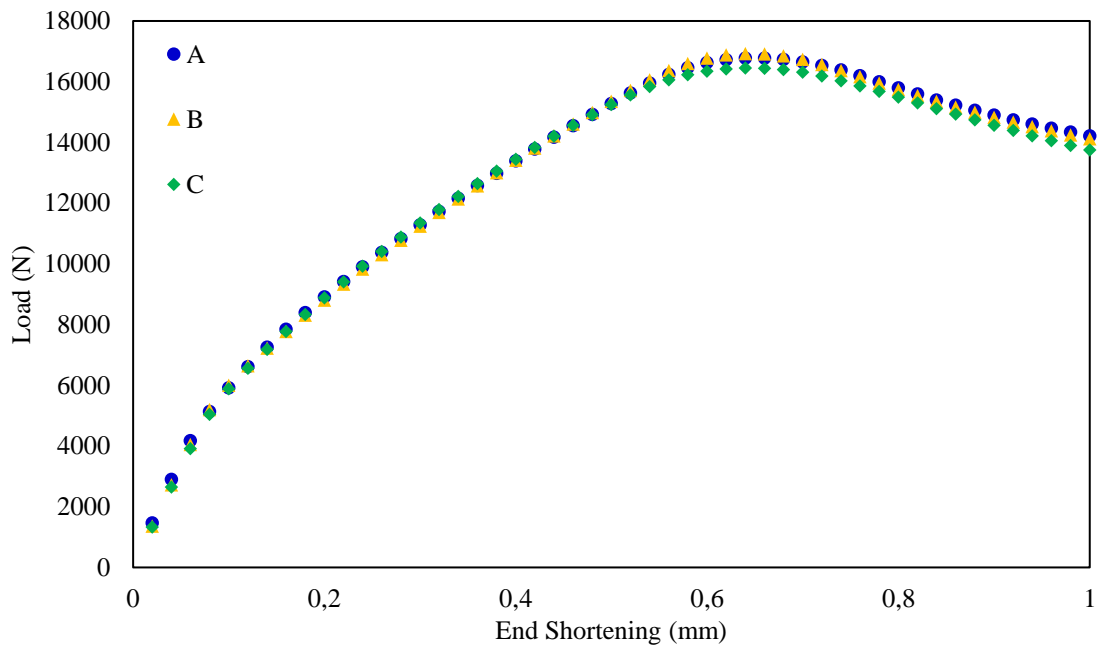


Fig. 6. Comparison of load-end shortening curves for models A, B, and C

Conclusion

Buckling represents a significant factor affecting structural stability and is a critical design parameter, particularly in the context of thin-walled structures. The buckling capacity of structures is contingent upon not only the material properties but also the geometric parameters. Accordingly, the impact of geometric variables, including curvature angle and upper surface width, on the buckling behavior of structures has prompted the present investigation. In this study, the buckling behaviors of hat-shaped structural

elements, modeled using aluminum alloy NL with varying geometric properties, have been investigated in detail. The findings of the study can be summarized as follows:

- Structures with a large curvature angle demonstrate a more uniform buckling behavior, whereas models with a low curvature angle exhibit more intricate and localized deformations.
- The results of the analyses conducted on hat-shaped structural elements with different curvature angles

demonstrate that the curvature angle has a significant influence on both the buckling load and the post-buckling behavior.

- In the initial three modes, Model C displays the highest buckling loads. However, as the mode number increases, Model B demonstrates a more balanced performance. This suggests that the influence of curvature angle on buckling loads is mode-dependent.

- As the modes progress, it has been determined that Model A's wider curvature angle distributes the buckling load more uniformly, thereby enabling it to withstand higher buckling loads.

- In the post-buckling analyses conducted, the load-deformation curves obtained for the three models exhibited similarities. Despite the presence of geometric differences, all models demonstrated linear behavior up to approximately 4000 N, followed by a nonlinear transition. While minor deviations in peak load values were observed due to slight differences in curvature angle, the overall behaviors remained largely similar.

The findings of this study offer substantial insights with practical implications for engineering disciplines such as aeronautical and automotive engineering. In particular, within the field of aviation, the optimization of curvature angle has the potential to facilitate the creation of aircraft fuselages and wing structures that are both lightweight and durable. In the automotive industry, the determination of design parameters with the objective of enhancing energy absorption capacity can be of paramount importance with regard to crash safety.

References

- [1] B. G. Falzon, "The behaviour of damage tolerant hat-stiffened composite panels loaded in uniaxial compression," *Compos. Part A Appl. Sci. Manuf.*, vol. 32, no. 9, pp. 1255–1262, 2001, doi: [https://doi.org/10.1016/S1359-835X\(01\)00074-4](https://doi.org/10.1016/S1359-835X(01)00074-4).
- [2] B. G. Prusty, "Free vibration and buckling response of hat-stiffened composite panels under general loading," *Int. J. Mech. Sci.*, vol. 50, no. 8, pp. 1326–1333, 2008, doi: <https://doi.org/10.1016/j.ijmecsci.2008.03.003>.
- [3] A. Nagesh, O. Rashwan, and M. Abu-Ayyad, "Optimization of the Composite Airplane Fuselage for an Optimum Structural Integrity." Nov. 09, 2018. doi: 10.1115/IMECE2018-88215.
- [4] E. G. Koricho and G. Belingardi, "An experimental and finite element study of the transverse bending behaviour of CFRP composite T-joints in vehicle structures," *Compos. Part B Eng.*, vol. 79, pp. 430–443, 2015, doi: <https://doi.org/10.1016/j.compositesb.2015.05.002>.
- [5] W. Hou, X. Xu, H. Wang, and L. Tong, "Bending behavior of single hat-shaped composite T-joints under out-of-plane loading for lightweight automobile structures," *J. Reinf. Plast. Compos.*, vol. 37, no. 12, pp. 808–823, Apr. 2018, doi: [10.1177/0731684418764608](https://doi.org/10.1177/0731684418764608).
- [6] W. Hou, X. Xu, X. Han, H. Wang, and L. Tong, "Multi-objective and multi-constraint design optimization for hat-shaped composite T-joints in automobiles," *Thin-Walled Struct.*, vol. 143, p. 106232, 2019, doi: <https://doi.org/10.1016/j.tws.2019.106232>.
- [7] S. Mesmoudi, M. Rammene, Y. Hilali, O. Askour, and O. Bourihane, "Variable RPIM and HOCM coupling for non-linear buckling and post-buckling analysis of transverse FG sandwich beams," *Structures*, vol. 53, pp. 895–907, 2023, doi: <https://doi.org/10.1016/j.istruc.2023.04.103>.
- [8] P. Hao, K. Zhang, D. Liu, X. Wang, S. Feng, and B. Wang, "Intelligent design and buckling experiment of curvilinearly stiffened thin-walled structures," *Int. J. Solids Struct.*, vol. 293, p. 112737, 2024, doi: <https://doi.org/10.1016/j.ijsolstr.2024.112737>.
- [9] S. Nadeem Masood, S. R. Viswamurthy, and K. M. Gaddikeri, "Composites airframe panel design for post-buckling – An experimental investigation," *Compos. Struct.*, vol. 241, p. 112104, 2020, doi: <https://doi.org/10.1016/j.compstruct.2020.112104>.
- [10] X. Liu, K. Han, R. Bai, Z. Lei, and H. Wang, "Buckling measurement and numerical analysis of M-type ribs stiffened composite panel," *Thin-Walled Struct.*, vol. 85, pp. 117–124, 2014, doi: <https://doi.org/10.1016/j.tws.2014.08.008>.
- [11] Y. Wang, F. Wang, S. Jia, and Z. Yue, "Experimental and numerical studies on the stability behavior of composite panels stiffened by tilting hat-stringers," *Compos. Struct.*, vol. 174, pp. 187–195, 2017, doi: <https://doi.org/10.1016/j.compstruct.2017.04.039>.
- [12] W. Hou, X. Xu, L. Sang, and L. Tong, "Failure of single hat-shaped thin-walled tubular composite T-joints under impact loading," *Thin-Walled Struct.*, vol. 154, p. 106815, 2020, doi: <https://doi.org/10.1016/j.tws.2020.106815>.
- [13] Y. Mo, D. Ge, and B. He, "Experiment and optimization of the hat-stringer-stiffened composite panels under axial compression," *Compos. Part B Eng.*, vol. 84, pp. 285–293, 2016, doi: <https://doi.org/10.1016/j.compositesb.2015.08.039>.
- [14] M. Albayrak, M. O. Kaman, and I. Bozkurt, "Experimental and Numerical Investigation of the Geometrical Effect on Low Velocity Impact Behavior for Curved Composites with a Rubber Interlayer," *Appl. Compos. Mater.*, vol. 30, no. 2, pp. 507–538, 2023, doi: [10.1007/s10443-022-10094-5](https://doi.org/10.1007/s10443-022-10094-5).
- [15] "ANSYS Academic Release 2020, Workbench Material Library."